LATE ORBITAL INSTABILITIES IN THE OUTER PLANETS INDUCED BY INTERACTION WITH A SELF-GRAVITATING PLANETESIMAL DISK

Harold F. Levison[1], Alessandro Morbidelli[2], Kleomenis Tsiganis[3], David Nesvorný[1], and Rodney Gomes[4]

[1] Southwest Research Institute, Boulder, CO 80302, USA; hal@boulder.swri.edu
[2] Departement Cassiopée, Universite de Nice-Sophia Antipolis, Observatoire de la Côte d'Azur, CNRS 4, 06304 Nice, France
[3] Section of Astrophysics, Astronomy & Mechanics, Department of Physics, Aristotle University of Thessaloniki, GR 54124 Thessaloniki, Greece
[4] Observatório Nacional/MCT, Rio de Janeiro, RJ, Brazil

ABSTRACT

We revisit the issue of the cause of the dynamical instability during the so-called Nice model, which describes the early dynamical evolution of the giant planets. In particular, we address the problem of the interaction of planets with a distant planetesimal disk in the time interval between the dispersal of the proto-solar nebula and the instability. In contrast to previous works, we assume that the inner edge of the planetesimal disk is several AUs beyond the orbit of the outermost planet, so that no close encounters between planets and planetesimals occur. Moreover, we model the disk's viscous stirring, induced by the presence of embedded Pluto-sized objects. The four outer planets are assumed to be initially locked in a multi-resonant state that most likely resulted from a preceding phase of gas-driven migration. We show that viscous stirring leads to an irreversible exchange of energy between a planet and a planetesimal disk even in the absence of close encounters between the planet and disk particles. The process is mainly driven by the most eccentric planet, which is the inner ice giant in the case studied here. In isolation, this would cause this ice giant to migrate inward. However, because it is locked in resonance with Saturn, its eccentricity increases due to adiabatic invariance. During this process, the system crosses many weak secular resonances—many of which can disrupt the mean motion resonance and make the planetary system unstable. We argue that this basic dynamical process would work in many generic multi-resonant systems—forcing a good fraction of them to become unstable. Because the energy exchange proceeds at a very slow pace, the instability manifests itself late, on a timescale consistent with the epoch of the late heavy bombardment ($\sim$700 Myr). In the migration mechanism presented here, the instability time is much less sensitive to the properties of the planetesimal disk (particularly the location of its inner edge) than in the classic Nice model mechanism.

Key words: planets and satellites: dynamical evolution and stability – planets and satellites: formation

1. INTRODUCTION

In 2005, a new model was published describing the early dynamical evolution of the solar system (Tsiganis et al. 2005; Morbidelli et al. 2005; Gomes et al. 2005), which has since come to be known as the Nice model. The Nice model is compelling because it explains many of the heretofore mysterious characteristics of the structure of the solar system. For example, it parks all four planets on orbits with separations, eccentricities, and inclinations similar to what we currently observe (Tsiganis et al. 2005), as well as duplicating the correct secular frequencies (Morbidelli et al. 2009a). In addition, it is the most successful model to date in explaining both Jupiter's (Morbidelli et al. 2005) and Neptune's Trojan asteroids (Tsiganis et al. 2005; Sheppard & Trujillo 2010). It reproduces the number and the inclination distribution of irregular satellites of the giant planets (Nesvorný et al. 2007; Bottke et al. 2010). It is the only migration model that is consistent with the current dynamical structure of the terrestrial planets (Brasser et al. 2009) and the main asteroid belt (Morbidelli et al. 2010). It may explain the origin of D-type main belt asteroids as objects that originally formed beyond the outer planets and were captured during planet migration (Levison et al. 2009). It reproduces many of the features of the dynamical structure of the Kuiper Belt, including the observed edge at $\sim$50 AU and the current Kuiper Belt mass (Levison et al. 2008). The Nice model (Gomes et al. 2005) reproduces the magnitude and the duration of the so-called Lunar late heavy bombardment (LHB; see Hartmann et al. 2000 for a review), which was a brief period of intense bombardment of

the inner solar system that occurred about 3.8 Gyr ago. Recent work by Barr & Canup (2010) suggests that, in the framework of the Nice model, the LHB would have delivered enough energy via impacts to differentiate Ganymede, but not Callisto, potentially explaining the observed differences between these bodies.

The Nice model is the latest and most developed of a class of models in which the giant planets are initially in a more compact configuration and achieve their current orbits through a phase of dynamical instability followed by a period of dynamical damping due to a planetesimal disk (Thommes et al. 1999, 2003; Levison et al. 2004). In the Nice model, the giant planets are assumed to have formed within 15 AU of the Sun. Slow migration was induced in the planets by gravitational close encounters with planetesimals, gradually leaking out of a $\sim$35 $M_\oplus$ primordial, trans-planetary planetesimal disk, set between $\sim$16 and 30 AU. After roughly 700 Myr, Jupiter and Saturn crossed their mutual 1:2 mean motion resonance (MMR). This event triggered a global instability that led to a violent reorganization of the outer solar system. Uranus and Neptune quickly evolved into orbits that crossed one another, as well as those of the gas giants. The ice giants penetrated the trans-planetary disk, scattering its inhabitants throughout the solar system. The interactions between the ice giants and the planetesimals damped the eccentricities and inclinations of the planetary orbits—leading the planets to nearly circular orbits at their observed locations. A small fraction of disk particles was trapped in the small body reservoirs, described in the previous paragraph.

While powerful, in our view, the Nice model as it was originally envisioned suffers from three main limitations. First, the initial orbits of the giant planets in the published Nice model simulations were chosen in an ad hoc manner. In particular, because no other information was available at the time, we simply placed all four planets on circular orbits, assuming that Saturn was closer to Jupiter than their mutual 1:2 MMR. The ice giants were then added with as small as possible spacing in semi-major axes that would still keep the system stable on billion year timescales. (It should be kept in mind that our goal was to drive otherwise stable planetary systems unstable by inducing planetesimal-driven migration due to small bodies leaking out of a distant planetesimal disk.) However, because we felt that the choice of initial conditions was a serious limitation of the model, in Morbidelli et al. (2007) we performed a comprehensive study of the dynamical evolution of the four giant planets embedded in a gas disk, in an attempt to determine realistic initial conditions for a new set of Nicelike simulations.

We found that the system naturally evolves into a configuration in which the planets are locked in a quadruple MMR (i.e., each planet is in resonance with its immediate neighbor or neighbors), similar to the Laplace resonance of the Galilean satellites. In total, we found four configurations in which the planets were stable for at least 1 Gyr after the disappearance of the gas.[5] Additional stable configurations were recently identified by Batygin & Brown (2010). In all our systems, Jupiter and Saturn are locked in the 2:3 MMR with one another. This arrangement seems to be the natural end state of the early dynamical evolution of the Jupiter–Saturn system embedded in a gas disk, even if one accounts for various accretion histories of Saturn (Pierens & Nelson 2008) and different structures of the disk (as long as they are reasonable; Zhang & Zhou 2010).

With these new multi-resonant configurations in hand, Morbidelli et al. (2007) and Batygin & Brown (2010) followed their evolution under the influence of a planetesimal disk. They showed that, as with the original Nice model, many of these systems became unstable and evolved into orbital configurations similar to that of the real giant planets. Thus, the first limitation of the Nice model appears to have been successfully addressed.

The second of the Nice model's limitations has to do with producing the delay in the onset of the instability that is required if the model is to explain the LHB (roughly 600 Myr). Recall that, in the original Nice model papers, the approach to the resonant crossing that led to instability was caused by the slow migration of the giant planets, due to the leakage of particles from near the inner edge of the disk. The migration was sustained by a feedback mechanism—particles leaking out of the disk would cause the ice giants to migrate outward, which, in turn, destabilizes additional particles from further out in the disk. It turns out that the exact value of the instability time was very sensitive to the location of the disk edge. In the original Nice model, we found that in order for the instability to occur between 200 Myr and 1 Gyr, the inner disk edge must lie between ∼14.5 and ∼15.5 AU, a range of only 1 AU. While not out of the question (see Gomes et al. 2005 for a discussion), this narrow range is aesthetically displeasing.

Moreover, the above problem is substantially worse for the configurations found by Morbidelli et al. (2007) because the planetary resonances destroy the feedback mechanism. As described above, in the original Nice model configuration, particles leaving the disk will cause the planets to change their semi-major axes. However, when the planets are in resonance, the leakage causes their eccentricities to decrease while leaving their semi-major axes virtually unchanged. Thus, as long as the planets remain in resonance, the outermost planet cannot move outward while the inner part of the planetesimal disk is dynamically eroded thereby making it much more likely that the process will stall, leaving the planets forever in their stable resonant configuration.

The third limitation in the original Nice model simulations was in the way we represented the planetesimal disk. In particular, in order for the problem to be computationally tractable, we ignored gravitational encounters (i.e., viscous stirring) between disk particles. Thus, during the long period of time that preceded instability, the disk remained significantly dynamically "colder" than it otherwise should have. This lack of viscous stirring is problematic when one considers that: (1) this disk probably contained on the order of 1000 Pluto-mass objects (Morbidelli et al. 2009b; Levison et al. 2008; Stern 1991), (2) the escape velocity of Pluto is ∼1 km s^{-1}, and (3) the orbital velocity in the middle of the disk is 6 km s^{-1}. Given these numbers, one would expect that Pluto-mass objects could excite the disk to eccentricities of ∼0.2. The fact that we did not include viscous stirring in our previous calculations is thus troubling, since a dynamically excited disk would probably be more effective at passing disk material to the planets. Thus, we must wonder whether it would still be possible to delay the instability for as long as ∼700 Myr, if viscous stirring were included. On the positive side, it is possible that the addition of viscous stirring would broaden the range of inner disk edge radii that lead to reasonably long delays, thereby solving the aesthetic problem above.

In response to the above issues, here we present the results of a new set of dynamical models, which start with a set of initial planetary orbits taken from Morbidelli et al. (2007), and include viscous stirring due to a population of Pluto-mass objects. Surprisingly, as we describe in Section 3.1, we find that viscous stirring leads to a heretofore unknown dynamical coupling between the planets and the disk, which in turn gives rise to a new trigger for the instability. Hereafter, we name this new model, characterized by resonant initial conditions for the planets and the new instability trigger as the "Nice II model."

The purpose of the present paper is to analyze the dynamics behind this newly discovered planet–disk coupling as well as to explore the relation between the instability time and the parameters of the model. We focus on one specific resonant orbital configuration of the planets, but we argue that the energy-exchange mechanism between planets and disk is generic. In Section 2, we discuss the methods we employed. In Section 3, we present the results of our simulations along with an interpretation for the observed dynamical coupling between the self-stirring disk and the planets. We show that this coupling can drive some systems unstable, but only after several hundred million years have elapsed. Our conclusions are given in Section 4.

---

[5] In the published version of Morbidelli et al. (2007), we claimed to have found only two stable configurations of the giant planets. Unfortunately, to test the stability, we used the original version of SyMBA (Duncan et al. 1998), which, as we discuss in more detail in Section 2, has a problem with integrating very compact planetary configurations for long periods of time. After fixing this problem, we find that four out of the six configurations identified by Morbidelli et al. (2007) are stable.

2. THE CALCULATIONS

For the Nice II model, we start with a system where the planets are in one of the configurations described by Morbidelli et al. (2007) and Jupiter's initial semi-major axis, a, is set to 5.4 AU.

Table 1
Time-averaged Elements[a] of the Four Giant Planets,
as Found in Morbidelli et al. (2007)

Planet	$\langle a \rangle$ (AU)	$\langle e \rangle$	$\langle i \rangle$ (deg)
Jupiter	5.42	0.0044	0.016
Saturn	7.32	0.017	0.016
Ice I	9.61	0.053	0.044
Ice II	11.67	0.011	0.029

Notes. This is the solution corresponding to a multi-resonant configuration in which Saturn is in a 3:2 MMR with Jupiter, Ice I is in a 3:2 MMR with Saturn, and Ice II is in a 4:3 MMR with Ice I. Note that the eccentricity of the inner ice giant (in 3:2 with Saturn) is much higher than that of the other planets.
[a] a, semi-major axis; e, eccentricity; and i, inclination.

In particular, we chose the system where Saturn (at ∼7.3 AU) is in the 2:3 MMR with Jupiter, the inner ice giant (hereafter *Ice I*, at ∼9.6 AU) is in the 2:3 MMR with Saturn, and the outer ice giant (hereafter Ice II, at ∼11.7 AU) is in the 3:4 MMR with Ice I. Jupiter and Saturn have their real masses, while both ice giants were given a mass equal to 15 $M_\oplus$. The time-averaged orbital elements of this initial system are given in Table 1. These were determined by integrating the planetary system for 1 Myr. Note for future reference that Ice I has a significantly larger eccentricity (∼0.05) than the rest of the planets (∼0.01). This is a common feature for all multi-resonant configurations found by Morbidelli et al. and Batygin & Brown (2010). We discuss the implications of this result below.

As stated above, in addition to the giant planets, our simulations include a massive particle disk, initially consisting of $N_{\rm disk}$ (usually 1500) equal-mass bodies, distributed so that the surface density scales with heliocentric distance as $\Sigma \propto r^{-1}$. The total mass of the disk ($M_{\rm disk}$) and the disk's inner edge ($r_{\rm in}$) are free parameters of this model. For most of our simulations we used a 50 $M_\oplus$ disk, as did Morbidelli et al. (2007) and Batygin & Brown (2010), which is slightly more than the nominal value of 35 $M_\oplus$ in the original Nice simulations (Tsiganis et al. 2005). Note that our standard configuration implies that the mass of an individual disk particle ($m_{\rm d} = M_{\rm disk}/N_{\rm disk}$) is roughly twice that of the Moon. Thus, each of these objects should be thought of as representing a swarm of real disk particles at similar positions and velocities. We also varied the outer edge of the disk ($r_{\rm out}$) so that runs with the same initial disk mass also had the same value of surface density within the disk. Our runs had outer disk edges that ranged from 30 to 34 AU. We truncate the disk near 30 AU to ensure that Neptune does not migrate too far (see Gomes et al. 2004 and Levison et al. 2008 for justifications of this). As in the original Nice-model simulations, the initial eccentricities and inclinations of disk particles are very small ($e \sim \sin(i) \sim 10^{-3}$).

The dynamical evolution of these systems was followed using a version of the symplectic N-body code known as SyMBA (Duncan et al. 1998). This code has been modified in three ways. First, SyMBA is a multiple time step algorithm, which makes use of a so-called transition function to symplectically change the time step of the integration. This function must be smooth, but also must not use a lot of CPU time. Duncan et al. (1998) advocated using a fourth-order polynomial for this purpose. While sufficient for most applications, we find that the integrator fails when trying to integrate, for long periods of time, systems where the planets pass within three mutual Hill radii of one another in each synodic period, as is the case for the compact configurations studied here. Thus, for the present simulations, we have adopted the transition function suggested
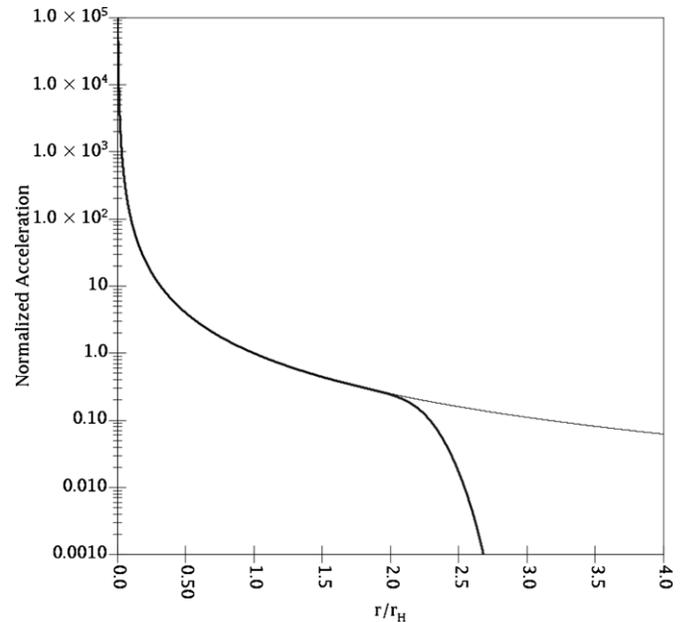

Figure 1. Normalized acceleration felt by one particle due to the gravitational interaction with another, as a function of r/r_H. The light gray curve is of the Newtonian functional form ($\sim 1/r^2$), while the solid curve is the one given by Equations (1) and (2). Note that the acceleration dies out quite quickly, for $r/r_H > 2$.

by Rauch & Holman (1999), which does not suffer from this problem.

While the self-gravity of the disk was ignored in the original Nice model runs, for reasons described above, we must now include viscous stirring. Unfortunately, it is still computationally too expensive to include the full gravitational interaction of the disk particles in a direct N-body integration. Thus, we needed to develop a simplified algorithm that includes the interactions, at least approximately, while being computationally efficient. We first tried the obvious strategy of occasionally kicking particles based on a simple particle-in-the-box algorithm. Unfortunately, these small kicks brake the symplecticity of the integrator and thus our planetary systems went unstable, even if the disk was placed very far from the planets.

Hence, the second modification to SyMBA is to include a new algorithm in which the magnitude of the acceleration that one disk particle feels due to the proximity of another is assumed to be of the form

$$a_d = \frac{Gm_p}{r_r^2} F(r_r; br_H, cr_H), \qquad (1)$$

where m_p is the mass of the perturber, r_r is the separation between the two objects, r_H is their mutual Hill's sphere, and b and c are dimensionless constants of order unity. The function F is 1 for $r_r < br_H$, 0 for $r_r > cr_H$, and smoothly and monotonically transitions between 1 and 0 in between. In particular, we again turned to the transition function developed by Rauch & Holman (1999), where for $br_H < r_r < cr_H$,

$$F \equiv \frac{1}{2}\left\{1 + \tanh\left[\frac{2y-1}{y(1-y)}\right]\right\}, \qquad (2)$$

where $y \equiv (r_r - br_H)/(cr_H - br_H)$. For these runs we set $b = 1.5$ and $c = 3.1$ in order to be consistent with the time step transitions in SyMBA. Figure 1 shows the functional form of the modified acceleration. With this form, we can ignore

3

the gravitational interaction between disk particles that are far from one another (thereby making the calculations much less computationally expensive), while symplectically integrating all close encounters between them.

The third and final modification to SyMBA comes from the fact that we have two different requirements on the way in which we represent the disk in our calculations. First, in order to correctly calculate the gravitational acceleration of the disk on the planets, we need to assume that the particles have a mass, m_d, that, in order to keep N_{disk} at a manageably small number, is on the order of the mass of the Moon. On the other hand, we want the disk to dynamically evolve due to viscous stirring as if it contains N_p objects of mass m_p, which is on the order of the mass of Pluto. So, in general $N_p < N_{disk}$ and $m_p < m_d$. Fortunately, there is nothing in the Hamiltonian formalism of this problem that requires that we set these two pairs of numbers equal to one another. In particular, when computing their effects onto the planets, we assume that the particles have all the same mass m_d; instead, when computing the mutual effects of planetesimals in the disk, we assume that N_p particles have a mass m_p while the remaining $(N_{disk} - N_p)$ particles have no mass (or more specifically they have mass $m_t \longrightarrow 0$). We can replace the potential part of the Hamiltonian with

$$\sum_{i=1}^{N_{pl}-1} \sum_{j=i+1}^{N_{pl}} \frac{Gm_i m_j}{r_{ij}} + \sum_{i=1}^{N_{pl}} \sum_{k=1}^{N_{disk}} \frac{Gm_i m_d}{r_{ik}}$$
$$+ \sum_{l=1}^{N_p-1} \sum_{\iota=l+1}^{N_p} \frac{Gm_p^2}{r_{l\iota}} + \sum_{\lambda=1}^{N_{disk}-N_p} \sum_{l=1}^{N_p} \frac{Gm_t m_p}{r_{l\lambda}}, \qquad (3)$$

where r_{ik} is the distance between particles i and j, and N_{pl} is the number of planets in the system. The physically meaningful free parameters in our simulations are r_{in}, M_{disk}, m_p, and N_p.

We have carefully tested this algorithm and it is working properly. In particular, the planets remain stable for longer than 4 Gyr when exposed to a disk containing 1000 Pluto-mass objects that are located very far from the planets. In addition, it is critical that the viscous stirring that occurs in our new code is comparable to that in a full N-body simulation. To test this, we performed three 1 Myr long integrations of a system containing the four giant planets in our chosen resonant configuration, surrounded by a disk containing 1000 objects of 14 $M_{\leftmoon}$ (i.e., $\approx 35\ M_\oplus$) spread from 14 to 30 AU. Figure 2 shows the root-mean-square (rms) eccentricity of the disk particles as a function of time in a full N-body simulation (dotted curve), our new code (solid curve), and a code that ignores self-gravity in the disk (light gray curve). The fact that the simulation with no self-gravity shows no trend indicates that the growth seen in the other two cases is due to viscous stirring and not due to the planets. Moreover, there is fairly good agreement between the full N-body results and that of our new code. The mean e^2 grows approximately linearly with time, with the growth rates of the two runs having a relative difference of $\sim 15\%$. The small discrepancy, we believe, is due to the lack of distant encounters. Given its small value and that m_p is a free parameter of our model, we believe that the agreement is adequate. We address the issue of the appropriateness of our methods again at the end of Section 3.1.

3. SIMULATION RESULTS

As described in the previous sections, our simulations follow the evolution of a system containing the four giant planets
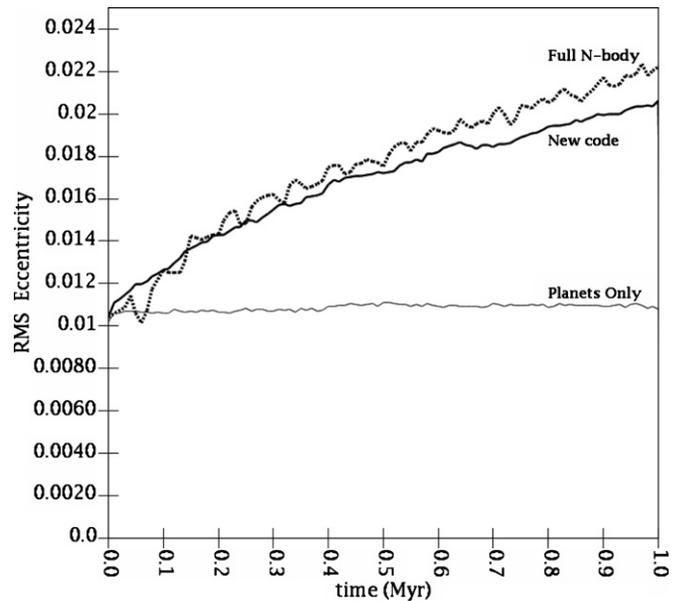

Figure 2. Growth in rms eccentricity in a disk spread from 14 to 30 AU that consists of 1000 objects of 14 Pluto masses and surrounds the four giant planets in our chosen resonant configuration. The dotted and heavy solid curves show the results obtained by a full N-body interaction and our new code, respectively. For comparison, the light solid curve shows what occurs when the disk does not contain any massive objects.

in a multi-resonant configuration, surrounded by a massive planetesimal disk. The disk has an inner edge at r_{in}, an outer edge at r_{out}, and a mass of M_{disk}. However, there is a relationship between these three values so that runs with the same M_{disk} had the same value of surface density within the disk as we varied r_{in}. The disk is stirred by a population of N_p objects with mass m_p. In the following section we describe the results of our simulations, starting with the discovery of a new dynamical coupling between the planets and a viscously stirred disk.

3.1. The Dynamical Coupling between the Planets and Disk

In the original Nice model simulations, the orbits of the giant planets changed as a result of close gravitational encounters with disk particles that were slowly leaking out of the disk. This leakage was due to the eccentricity growth that disk particles suffer when in MMRs with the planets. Thus, here we expected to see no change in the orbits of the giant planets in systems with r_{in} large enough that there was no leakage. We were surprised, therefore, to discover that in systems with viscous stirring, there exists a slow, secular transfer of energy from the disk to the planets.

The simulation shown in Figure 3 illustrates this point. The black curve shows the change in energy of the planets under the gravitational influence of a 50 $M_\oplus$ disk, spread between 18 and 31.6 AU. There were 1000 Pluto-mass objects embedded in the disk. As the figure shows, the planets are slowly being pushed toward the Sun ($\Delta E < 0$). At the same time energy is being pumped into the planetesimal disk (gray curve) in such a way that the total energy is constant. No particles leave the disk during this time. Indeed, the smallest perihelion distance any disk particle achieves is 15.7 AU, while all planets are inside of 12 AU.

The remainder of this section is devoted to describing the nature of this unexpected coupling. The first step is to confirm that it is indeed the result of adding viscous stirring to the problem and not some other effect, like that of the planetary
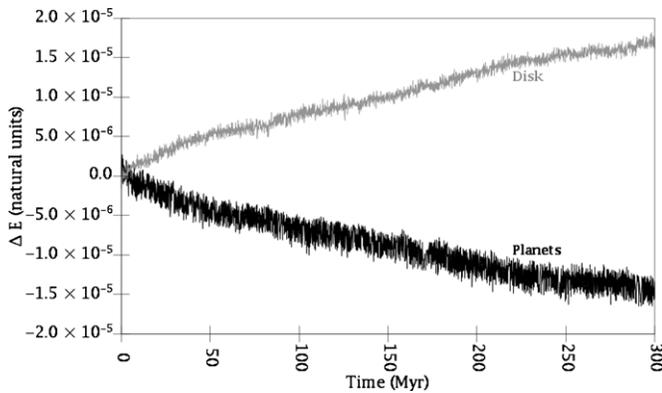
Figure 3. Change in total energy ($\Delta E = E - E_0$, E_0 is the initial value) contained in the four planets (sum of their two-body energies, black curve) and the disk particles (light gray curve) as a function of time. The energy drift is linear in time and has the same magnitude but opposite signs for these two components, so that the total energy of the system is conserved (no escaping particles; good behavior of the symplectic algorithm). Energy is given in what we call *natural units* where distance is measured in AUs, time in years, and the Sun's mass is equal to $4\pi^2$.

MMRs. In Figure 4(a) we plot the magnitude of the rate of change of the energy in the planets, $|dE/dt|$, as a function of N_p for systems with $M_{disk} = 50\,M_\oplus$, $r_{in} = 18$ AU, and $m_p = 1\,M_{\mathbb{P}}$. We see a nearly linear relationship between $|dE/dt|$ and N_p for $N_p \lesssim 500$. The fact that the energy drift decreases with N_p shows that the drift is mainly due to viscous stirring.[6]

The coupling saturates for N_p larger than ~500. This is potentiality the interesting region of our parameter space because we believe that the real trans-planetary disk should have contained on the order of 1000 Pluto-sized perturbers, for the following reason. Roughly 50% of the sky has been searched for Kuiper Belt Objects (KBOs) larger than 1000 km in radius, and two have been found: Pluto and Eris (Brown et al. 2005; Brown &

---

[6] We note that the energy drift does not go to zero when the number of scatterers goes to zero. We believe that this is the result of standard satellite/disk torques that are still present when $N_p = 0$ and are responsible, e.g., for gap opening in Saturn's rings (Goldreich & Tremaine 1980, 1982). This rate is, however, too small to significantly change the orbits of the giant planets over the age of the solar system.
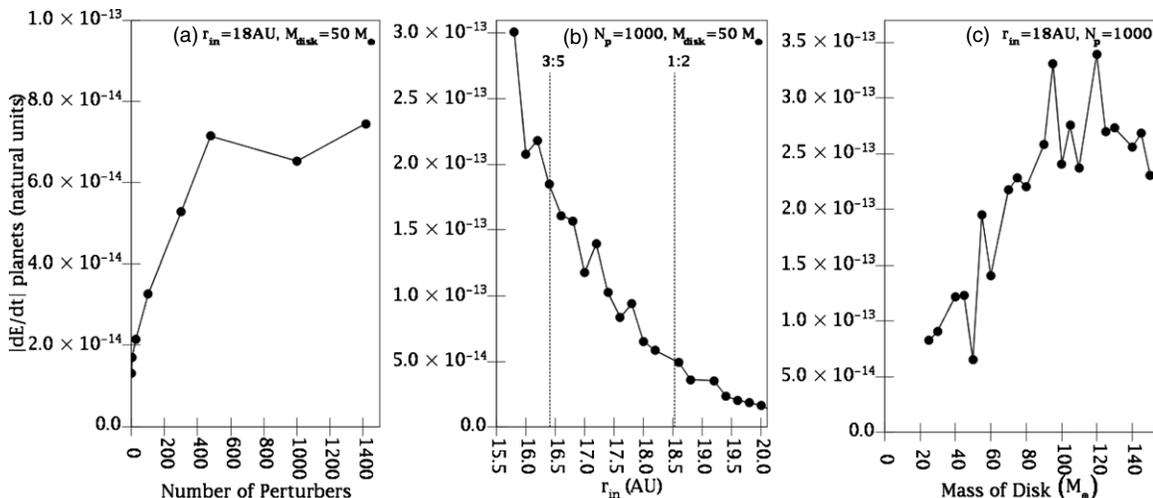
Schaller 2007). Levison et al. (2008) predict that 0.3%–0.6% of the protoplanetary disk should have been trapped in the Kuiper Belt during the instability phase of the planetary system. If four Pluto-sized objects indeed exist, then the original disk should have contained ~700–1300 such objects. Thus, adopting $N_p = 1000$ as our canonical value seems reasonable. The fact that we see $|dE/dt|$ saturating for $N_p \gtrsim 500$ implies that our results will not be sensitive to our choice of N_p, implying that we can effectively remove one degree of freedom from the model.

Because they play an important role in the original Nice model, the next question we need to address is whether MMRs are also important for the observed dynamical coupling. In Figure 4(b) we plot $|dE/dt|$ for a number of simulations where we fixed N_p and M_{disk}, but varied the inner edge of the disk, r_{in}. If MMRs were important for the observed energy coupling, we would expect jumps in $|dE/dt|$ as the edge of the disk passes over them (marked in the figure). Instead we see a smooth, monotonic decrease of $|dE/dt|$ with r_{in}. Therefore, we conclude that the MMRs are unlikely to play an important role in this new planet–disk coupling.

Figure 4(c) shows how the mass of the disk affects $|dE/dt|$. For $M_{disk} \lesssim 100\,M_\oplus$ the relationship is approximately linear. For larger disk masses, $|dE/dt|$ is apparently no longer monotonic in M_{disk}. We believe that this is due to the presence of nonlinear terms in the problem for these masses. Fortunately, we are most likely in the linear regime. In the original Nice-model simulations, we favored a disk mass of $35\,M_\oplus$, while the successful runs in Morbidelli et al. (2007) and Batygin & Brown (2010) employed $50 < M_{disk} < 91\,M_\oplus$. In any case, any explanation for our new coupling must explain this linear behavior.

Further insight into our coupling can be gained by investigating the behavior of the planetary orbits during these simulations. We find that the most obvious changes are seen in the orbit of the *inner* ice giant. Figure 5(a) shows that the eccentricity of Ice I (purple curve) increases substantially as a result of the energy coupling. In addition, the libration amplitude of the 3:4 MMR between the two ice giants increases during this period (Figure 5(b)). This occurs only if the coupling is pushing the two ice giants apart. These two observations suggest that the disk is pushing the orbit of Ice I inward, while leaving Ice II mainly
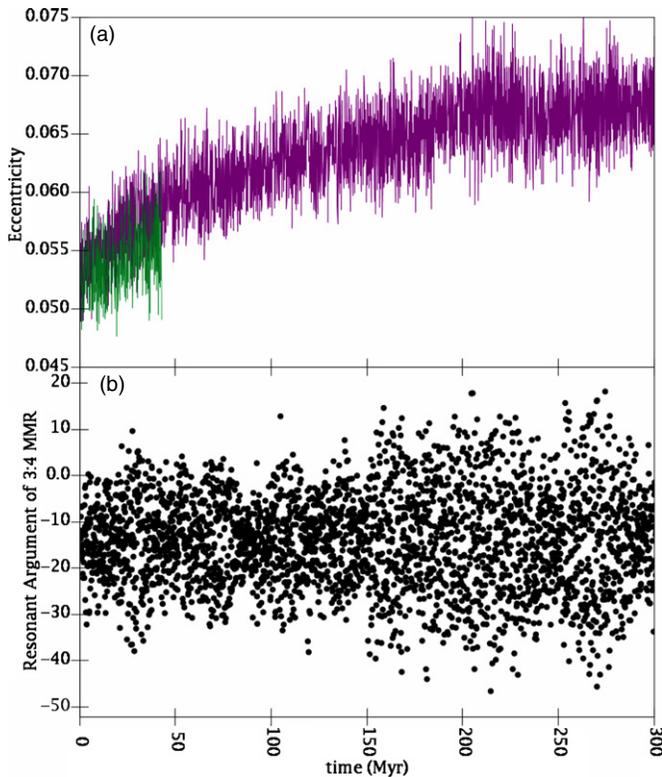

Figure 4. (a) Absolute value of dE/dt as a function of the number of perturbers, N_p. The inner edge of the $50\,M_\oplus$ disk was set to $r_{in} = 18$ AU. Note that $|dE/dt|$ saturates for $N_p \gtrsim 500$. (b) The same quantity as measured in a series of simulations with $N_p = 1000$ and different values of r_{in}. The observed monotonic dependence suggests that MMRs (noted in the plot) do not play an important role in the observed energy exchange. (c) $|dE/dt|$ as a function of the mass of the disk. All these simulations had $N_p = 1000$ and $r_{in} = 18$ AU. Note the linear dependence for $M_{disk} \lesssim 100\,M_\oplus$.

Figure 5. (a) Eccentricity evolution for Ice I for the run of Figure 3—purple curve—and the same for a run in which Ice II was removed—green curve. In both runs the eccentricity increases at roughly the same rate. (b) Time evolution of the critical angle related to the 3:4 MMR between Ice I and Ice II, for the run of Figure 3. The amplitude of libration increases as well.

unaffected. This naturally explains the change in the 3:4 libration amplitude. Also, Ice I's eccentricity increases because it is trapped in the 2:3 MMR with Saturn. This resonance prevents Ice I's semi-major axis from decreasing fast enough; Ice I needs to drag Jupiter and Saturn with it. Instead, as is well known from the dynamics of the Galilean satellites and the Kuiper Belt's plutinos, the preservation of an adiabatic invariant forces a slow *increase* of its orbital eccentricity that compensates for the slow drift in a (Henrard 1993; Peale 1986).

The hypothesis described in the last paragraph can be tested by performing a simulation similar to the one used to generate Figure 3 and the purple curve in Figure 5, but without Ice II. The green curve in Figure 5(a) shows the eccentricity of Ice I in this simulation. As can be seen, the eccentricity increases at roughly the same rate as in the original run. This result strongly suggests that the main coupling between the disk and the planets is through the inner ice giant. This is a surprising result, given that Ice I is much farther from the disk than Ice II. Recall, however, that Ice I has an initial eccentricity of 0.053, while the rest of the planets have eccentricities less than 0.017. Thus, in order for Ice I to play a decisive role, the dynamical mechanism responsible for the coupling must be a strong function of the eccentricity. Given the results thus far, we can infer that the observed energy exchange is related to secular interactions between the planets and the disk.

It may seem absurd that a secular interaction results in an energy exchange, but it turns out to be the case. It was Milani et al. (1986) that first noticed in their numerical integrations that the semi-major axes of the planets were exhibiting long-period oscillations, correlated to the evolution of their eccentricities. This was unexpected at the time, because it was thought that

the semi-major axes could have only short-periodic oscillations associated with the mean motion. This belief is, however, only approximately correct, as Milani et al. (1987) have analytically proved. In particular, they showed that, computing the relationship between the osculating and mean semi-major axes (the latter being constants of motion) using series expansions and rigorous perturbation techniques, one finds terms with amplitudes that are a function of the product of the masses of the interacting bodies and independent of their mean longitudes. This is because for every short-periodic term that one eliminates when averaging using canonical perturbation theory, a *higher-order* secular term has to be added in the expansion of the Hamiltonian as well as in the transformation equations between the new and old coordinates. As a result, the semi-major axes are not only a function of the mean longitudes, but of the secular angles as well. These additional terms may be small in amplitude, but describe secular oscillations of the osculating semi-major axes. Since the semi-major axes are, of course, related to the orbital energies of the planets, the latter have secular oscillations as well.

In short, Milani et al. (1987) demonstrated that, in the general case of two interacting massive bodies, the energy of the first body has a *secular* oscillation around its mean value. In general, this oscillation, to lowest order in the eccentricities, is given by the formula

$$E = \bar{E} + C_1 e^2 + C_2 e'^2 + C_3 e e' \cos(\varpi - \varpi'), \qquad (4)$$

where e and ϖ denote the mean-motion-averaged eccentricity and longitude of perihelion, and the primed quantities refer to the inner body. The C's are constants that depend, very sensitively, on the geometry of the system. For example, in the case of Uranus and Neptune in the current solar system, Uranus's energy is at minimum when its eccentricity is at minimum. However, if Neptune were to be placed on the other side of the 1:2 MMR with Uranus, the phase would shift and Uranus's energy would be at maximum when its eccentricity is at minimum.

In our case, the planets are interacting with a disk of planetesimals. If the planetesimals were not interacting with each other, the secular evolution of the energy of a planet would still be described by Equation (4), but with a sum over the unprimed quantities, denoting the collection of all disk particles. Hence, the energy of the planet would have a complicated, but still quasi-periodic evolution—given by the sum of many small-amplitude and long-period oscillations—but NO net drift.

However, when two disk particles gravitationally scatter one another, their ϖ and e suffer instantaneous changes that depend on the details of the encounter, and are unrelated to the secular forcing exerted by the planet. If the ensemble of disk particles undergoes a non-periodic drift, then we would expect the energy of the planet to change as well. In particular, it is well known that the addition of viscous stirring causes the rms eccentricity of the disk to increase with time (Figure 2). Since, according to Equation (4), E of the planet is a function of the eccentricity of the disk, it seems reasonable to investigate whether this is the culprit.

Unfortunately, it is not trivial to perform a direct comparison between Equation (4) and our systems. As mentioned above, computing the C's for each particle and adding their effects together would be extremely cumbersome. However, we can qualitatively compare the behavior of our systems to that predicted by this equation. The first step in this comparison is to note that, according to Milani et al. (1987), $|dE/dt|$ should roughly scale as $M_{\mathrm{Uranus}} \times M_{\mathrm{disk}}$ when Equation (4) is summed

over all the disk particles. Figure 4(c) shows that $|dE/dt|$ is indeed linear in $M_{\rm disk}$, confirming this prediction.

Next, Equation (4) shows that $|dE/dt|$ should be dependent on a combination of the eccentricities of the planet and the disk particles. Because the observed secular change in the orbital energy of the planets is clearly linked to changes in the disk caused by viscous stirring, we believe that the C_2 term in Equation (4) can be ignored. The C_1 term is independent of the eccentricity of the planet. So, since, as we described above, the strongest coupling between the planets and the disk is through Ice I, which has a large eccentricity, we conclude that in the framework of our theory, the third term in the equation must dominate in the case of interest here.

The next issue to address is whether after making the above conclusion, we can explain the behavior that we see. Defining a new angle $\phi \equiv (\varpi - \varpi')$, the change in energy of the planet as determined by the dominant C_3 term should be

$$\frac{dE}{dt} \propto \frac{de}{dt}e'\cos(\phi) + e\frac{de'}{dt}\cos(\phi) + ee'\sin(\phi)\frac{d\phi}{dt}. \quad (5)$$

We now estimate the magnitude of each term in this equation.

It is well known that an eccentric planet will try to force a population of non-interacting particles to be uniformly distributed around a single point in the h–k plane, where $h \equiv e\cos(\phi)$, and $k \equiv e\sin(\phi)$. This forced equilibrium lies on the h-axis at distance e_f from the origin, where e_f is known as the forced eccentricity. Therefore, once a quasi-equilibrium is set up in the disk, the average value of $\cos(\phi)$ for our disk particles should be a positive constant smaller than 1, while the average $\sin(\phi) \approx 0$. Thus, we can ignore the third term in Equation (5).

We next turn our attention to the eccentricities. Unfortunately, in our full simulations, the eccentricity of Ice I is contaminated by its MMR with Saturn. Thus, to help in this analysis we turn to more simplistic simulations. In particular, we ran three experiments in which we picked up one of our simulations at $t = 50$ Myr and continued the integration after removing all planets except Ice I (i.e., the system consisted of the Sun, Ice I, and the disk). The eccentricity of Ice I (equal to 0.054 after 50 Myr in our original simulation) is varied in the three experiments (0.02, 0.05, and 0.07). We observe, as expected, that the higher the initial eccentricity of Ice I, the faster its eccentricity damped and the faster the rms eccentricity of the disk's particles increased. In all cases, the semi-major axis of the planet decreased with a rate roughly proportional to the planet's initial eccentricity: $da/dt = -1.1 \times 10^{-11}$, -2.0×10^{-11}, and -3.6×10^{-11} AU yr^{-1} for initial $e' = 0.02$, 0.05, and 0.07, respectively. We deduce from these experiments that (1) *inward* migration of the planet is generic (which was unclear since we do not know the value, or even the sign, of C_3) and that (2) its magnitude linearly depends on the planet's eccentricity, which governs its secular coupling to the disk.

In addition, we find that the planetary energy drift in the simulation with only Ice I is the same as in the full simulation. In particular, recall that in the $e = 0.05$ run, we found that $da/dt = -2.0 \times 10^{-11}$. Since

$$\frac{dE}{dt} = \frac{GM_\odot M_{\rm Ura}}{2a^2}\frac{da}{dt},$$

$dE/dt = 1.5 \times 10^{-14}$ in natural units. In the full system, we find that $dE/dt = 1.6 \times 10^{-14}$ (this is the $r_{\rm in} = 20$ AU, $N_p = 1000$ run in Figure 4). This result is insightful because not only does

it confirm that the main coupling is through Ice I, but in our full runs de'/dt is positive ($\sim 5 \times 10^{-5}$ Myr^{-1}), while it is negative in these new runs ($\sim -3 \times 10^{-4}$ Myr^{-1} for the simulation with an initial eccentricity of 0.05). This, in turn, indicates that the first term in Equation (5) dominates. We can understand why this is the case by comparing the first and second terms in the equation. In this problem, $e_{\rm rms}$ and e' are of the same order. However, because of viscous stirring, $de_{\rm rms}/dt$, which has a value of roughly 2×10^{-3} Myr^{-1}, is at least an order of magnitude larger than de'/dt.

Thus, we conclude that $|dE/dt| \propto M_{\rm disk}de/dte'$, at least in the linear regime. According to the classic viscous stirring equations, de/dt is linear in the number density of scatterers (cf. Wetherill & Stewart 1993), which is proportional to N_p in our case. Thus, our analysis of Equations (4) and (5) suggests that dE/dt should be linear in N_p, e', and $M_{\rm disk}$, which is what we observe.

With this information in hand, we can now revisit the appropriateness of the simplifications we employ in our numerical techniques. As we describe in Section 2, we smoothly and symplectically truncate the force that the disk particles feel from the Pluto-mass objects at roughly $2r_H$ (see Figure 1) in order to decrease the amount of CPU time required for the calculations. There are two consequences of this simplification that affect $|dE/dt|$. First, we are missing distant, small angle encounters. This mainly will affect the growth of the eccentricities of the disk. As shown in Figure 2, our code handles this fairly well.

The second issue arises from the fact that the disk particles do not feel the bulk gravitational potential of the disk, and so their secular precession frequencies, and thus $d\phi/dt$, are in error. In order to test the importance of this we performed a calculation similar to the single planet simulations above, but we added a fixed gravitational potential corresponding to a $50\,M_\oplus$ disk spread from 18 to 34 AU with an r^{-1} profile. Ice I, which was the only planet in the simulation, had an initial eccentricity of 0.05. We found that it drifted inward at a rate of -3×10^{-11} AU yr^{-1}—only slightly larger than the value of $da/dt = -2 \times 10^{-11}$ AU yr^{-1} observed when the disk potential was not included. Given that changes in disk parameters have a much larger effect than this (see Figure 4), we feel this is an acceptable compromise. Thus, we can conclude that our simplifications are, indeed, valid for the problem at hand. Note that this exercise supports the above conclusion that the $d\phi/dt$ term in Equation (5) is unimportant.

One final note on this topic: although we studied only one of a large number of possible resonant configurations for the planets, we believe that the same basic behavior would occur in any multi-resonant configuration. Our study of an isolated planet shows that the energy coupling of an eccentric planet with a disk is generic. In addition, all of the planetary systems that have been produced thus far have at least one eccentric planet (Morbidelli et al. 2007; Batygin & Brown 2010). Indeed, in all resonant configurations found in Morbidelli et al. (who used hydrodynamic simulations and thus generated the most realistic systems), the most eccentric planet is Ice I, as is the case here. In all cases, the resonant locks between the planets will turn the energy decay into an eccentricity growth. Since $|dE/dt|$ is a function of the planet's eccentricity, this pumping sustains the coupling process. Thus, the same kind of evolution observed in Figures 3 and 4 should repeat whatever multi-resonant configuration the giant planets had at the time.
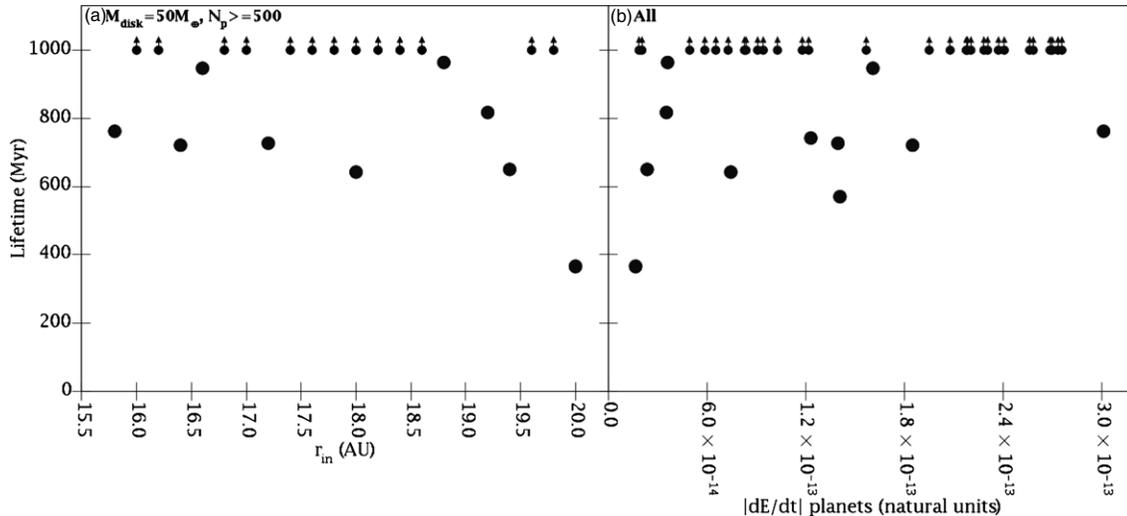
Figure 6. (a) The dynamical lifetime of systems, as a function of the inner edge of the disk. All runs are for a disk of 50 $M_\oplus$ and $N_p > 500$. (b) The dynamical lifetime of all the systems shown in Figure 4 as a function of $|dE/dt|$. The median lifetime of unstable systems is 730 Myr.

3.2. Leading to a Planet Orbital Instability

As described in Section 1, one of the main criticisms of the original Nice model was that the timing of the instability, and thus whether it could explain the LHB, was very sensitive to the choice of the inner edge of the disk. In particular, for $r_{in} \lesssim 14.5$ AU the system went unstable in a very short period of time, and yet if $r_{in} \gtrsim 15.5$ AU the system was stable for 1 Gyr. And so, although this limitation only affects one aspect of the Nice-model story, the only way for the Nice model can explain the LHB is for the disk to have an edge within a narrow region of the solar system.

The question naturally arises whether (1) the Nice II model can lead to late instability, and (2) it also suffers from the same limitation as the original Nice model. In order to test the sensitivity of the new model to r_{in}, we have plotted the dynamical lifetimes of the 22 simulations from Figure 4(b) that have $M_{disk} = 50\,M_\oplus$, $m_p = 1M_\leftmoon$, and $N_p > 500$, but r_{in} that ranged from 15.8 to 20 AU, in Figure 6(a). In particular, each dot represents one simulation. Small dots are systems that were stable for 1 Gyr, while large dots represent systems that became unstable. It is interesting to note that (1) the dynamical lifetime is not a monotonic function of r_{in} and, more importantly, (2) the systems that go unstable tend to have dynamical lifetimes that are close to the value needed to explain the LHB ($\sim$600 Myr after the solar system formed). Our unstable systems have dynamical lifetimes between 366 and 964 Myr, with a median of 730 million years. These late instabilities provide a natural explanation for the LHB. We return to the issue of the timescale below.

The fact that some systems remain stable while others do not was surprising to us. To understand this result, we must first understand what causes the instability. As explained above, planets should radially migrate due to the exchange of energy and angular momentum with the trans-planetary disk. Ice I, which has the largest eccentricity (0.053), exchanges far more energy/angular momentum with the disk and should therefore migrate faster than the other planets. Since it is locked in MMRs with Saturn and Jupiter, however, its orbital eccentricity should increase instead, which is exactly what we see in our simulations (Figure 5).

The eccentricity growth, in turn, causes the precession frequencies of the planetary system to slowly vary. This raises

the possibility that some of these frequencies become similar to one another, thereby giving rise to secular resonances. The perturbations induced by secular resonances can undermine the system's fragile mutli-resonant architecture by disrupting some of the resonant "locks" that hold the planets together. The system is doomed if that happens, because non-resonant systems as compact as ours (i.e., separated by only a few Hill radii) are naturally unstable if not locked in MMRs (Gladman 1993; Chambers et al. 1996).

An example of the typical unstable system is shown in Figure 7, which shows the evolution of Ice I's eccentricity and the critical argument of the 3:4 MMR between Ice I and Ice II ($\sigma_{I,II} \equiv 3\lambda_I - 4\lambda_{II} + \varpi_I$) immediately before the instability. As described above, initially Ice I's eccentricity is slowly increasing. However, at approximately 325 Myr, Ice I's eccentricity suddenly drops. This drop destroys the 3:4 MMR, which leads to instability. We believe that this drop is due to the crossing of a secular resonance.

We employed Fourier analysis of the orbital elements time series of the planets (Šidlichovský & Nesvorný 1996) to get insight into the nature of possible secular resonances crossings in our simulations. This analysis was complicated by the fact that the planetary orbits are strongly coupled. Thus, it was not clear which of the (many) peaks found in the time series of a given quantity corresponded to the fundamental mode of the given planet/element, which peaks were combinations of the fundamental modes, and which ones were "projected" into this element from other degrees of freedom. In addition, the presence of the disk, with its 1500 particles—each with its own secular frequencies—makes the analysis of our systems very challenging.

As a result, we decided to analyze a simpler system containing only Jupiter, Saturn, and Ice I; Ice II and the disk were removed. We mimicked the effects of the disk by adding a fictitious force to Ice I's equations of motion that slowly draws energy from its orbit (Malhotra 1995). We integrated the system for 1.5 Gyr. We found that Ice I suffered the sudden drop in eccentricity observed in our full simulations (as shown in Figure 7). Fortunately, this system did not suffer an instability (presumably because of the absence of Ice II), which allowed us to continue to study its evolution after the drop in e was observed.
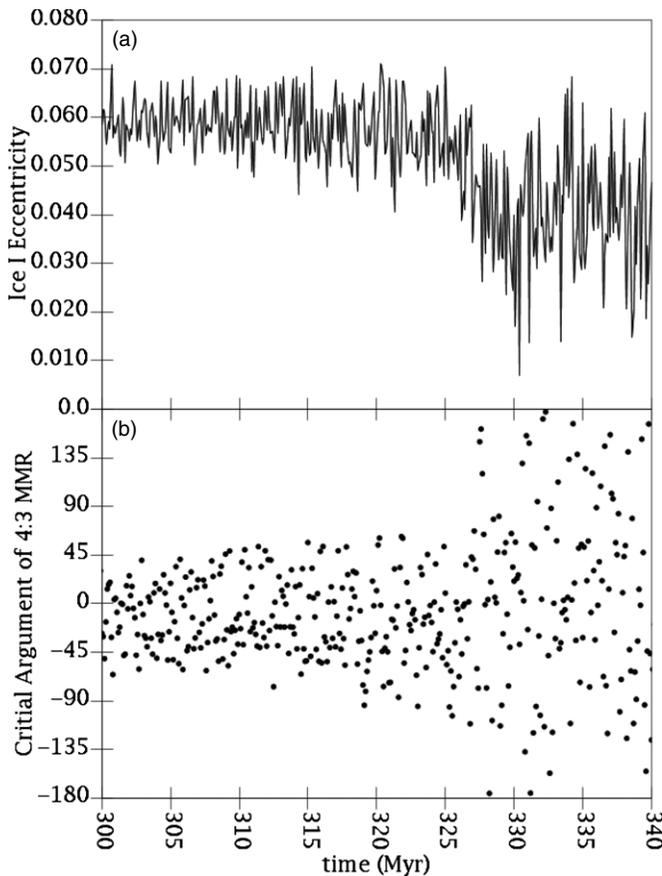
Figure 7. (a) Evolution of Ice I's eccentricity with time in the run with $N_p = 1000$, $M_{\mathrm{disk}} = 50\,M_\oplus$, and $r_{\mathrm{in}} = 20$ AU near the time of the instability observed in the full system. (b) The eccentricity drop seen at $t \approx 325$ Myr is correlated with a transition of the critical angle of the 3:4 MMR between the two ice giants from libration to circulation.

Figure 8. Time evolution of the arguments $\varpi_J - \varpi_S$ (top) and $\varpi_S - \varpi_{\mathrm{IceI}}$ (bottom), for the reduced planetary system described in the text. The initial condition corresponds to the run of Figure 7, ~47 Myr before the eccentricity drop occurred. As seen in these plots, the period of libration of $\varpi_J - \varpi_S$ is very close to the period of circulation of $\varpi_S - \varpi_{\mathrm{IceI}}$.

We determined the secular frequencies of this reduced planetary system at several different time snapshots: before, during, and after the eccentricity drop. This allowed us to judge which of the frequencies are drifting with time and which ones have similar values during the eccentricity drop, thus revealing the nature of the potentially destabilizing agent. In the case studied here, we found that the drop was caused by the crossing of a secular resonance produced by the beat between the libration of $\varpi_J - \varpi_S$ and the circulation of $\varpi_S - \varpi_{\mathrm{IceI}}$.

At the time shown in Figure 8, which corresponds to 47 Myr before the eccentricity drop, the period of $\varpi_J - \varpi_S$ ($P_{\varpi_J - \varpi_S}$) is slightly larger than that of $\varpi_S - \varpi_{\mathrm{IceI}}$ ($P_{\varpi_S - \varpi_{\mathrm{IceI}}}$)—178.3 and 172.6 yr, respectively. As e_{IceI} grows, $P_{\varpi_J - \varpi_S}$ decreases while $P_{\varpi_S - \varpi_{\mathrm{IceI}}}$ increases. Thus, these frequencies are on a collision course. In our reduced (stable) system we found that, 53 Myr after the eccentricity drop, $P_{\varpi_J - \varpi_S} = 171.7$ yr and $P_{\varpi_S - \varpi_{\mathrm{IceI}}} = 176.2$ yr. Hence, the secular resonance was crossed.

Before we can proceed, we must make sure that by removing Ice II from our system we have not oversimplified the problem. In particular, we need to make sure that the secular frequencies of the primary angles involved in the above resonance do not significantly change when Ice II is removed. We tested this by performing three experiments. Each of these started with an orbital configuration taken at 325 Myr, which is immediately before the time when Ice I's eccentricity dropped, from our full simulation shown in Figure 7. Each simulation consisted of a different system: (1) the four planets plus the disk particles (but
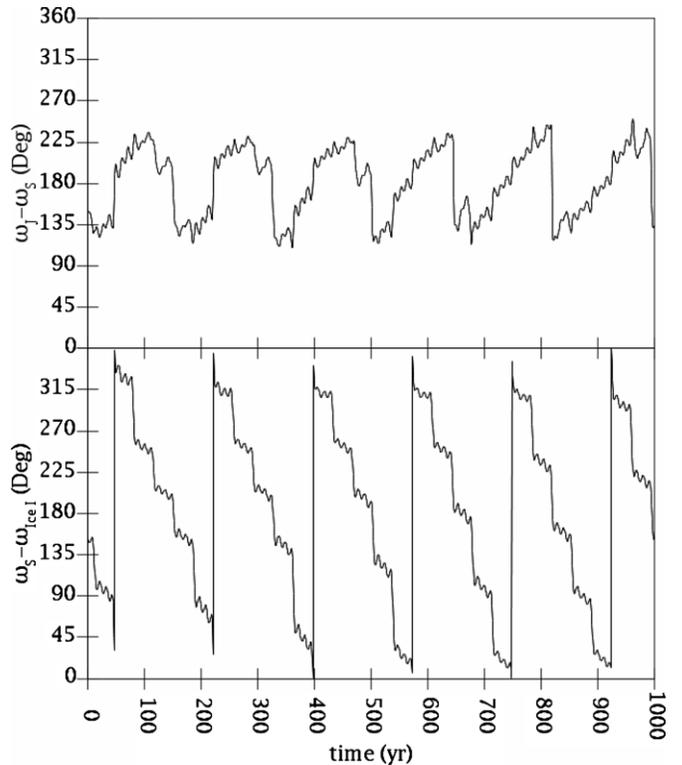
suppressing self-stirring), (2) the four planets without the disk, and (3) three planets only (removing Ice II). We find that the mean frequencies of $\varpi_J - \varpi_S$ and $\varpi_S - \varpi_{\mathrm{IceI}}$ vary by at most 2% between the runs. Hence, we are confident that what we see in our simplified three-planet model is not substantially different from the full system.

The above results lead us to conclude that the eccentricity drop seen in our full simulation is caused by the crossing of the secular resonance identified above. This, in turn, leads to an increase in the libration amplitude associated with the MMRs between the planets, as shown in Figure 7. Although we argue below that different secular resonances are involved in different runs, a similar drop in Ice I's eccentricity was observed in all our systems. In some cases, this causes the planets to break out of the MMRs, thereby forcing the system becoming unstable. However, in other runs, the MMRs are not disrupted by the secular resonance crossing. We believe that the difference is likely related to the different phases at the time the secular resonance is crossed.

While this argument naturally explains why some of our systems are stable and others are not, it does not explain the dynamical lifetimes we observe. Recall that we find that $|dE/dt|$ is a monotonically decreasing function of r_{in} (Figure 4(b)). If the identified secular resonance were responsible for all of our unstable systems, we would expect a relationship between the dynamical lifetime of our systems and $|dE/dt|$ because the smaller $|dE/dt|$ the longer it would take to reach the resonance. In Figure 6(b), we plot the dynamical lifetime of the 42 systems shown in Figure 4. Recall that these runs include systems with r_{in} between 15.8 and 20 AU and disk masses between 25 and 150 $M_\oplus$, and have $|dE/dt|$ that range over a factor of 30, yet

there is no apparent relationship between dynamical lifetime and $|dE/dt|$.

Therefore, we believe that the systems that evolve more slowly (i.e., smaller $|dE/dt|$) are destabilized by crossing different resonances that are weaker than the one described above, but are crossed more slowly. Recall that the effect of a resonance is not simply proportional to its strength (i.e., the magnitude of the coefficient of its related harmonic term), but increases if the resonance is crossed at a slower rate (up to some adiabatic limit). Therefore, it is possible that a resonance that does not have a significant effect when crossed at large $|dE/dt|$, will provide a strong change to the orbits, possibly leading to escape from the MMRs, if crossed at significantly smaller $|dE/dt|$.

The probability that a system will go unstable in a given time interval roughly scales as the number of potentially destabilizing resonances that are crossed. Since the weak resonances are more numerous than strong ones, the density of potentially destabilizing resonances increases as $|dE/dt|$ decreases, and so the number crossed in a given amount of time could be roughly independent of $|dE/dt|$. If true, we would not expect any strong relationship between the physical parameters in the model (which set $|dE/dt|$) and the dynamical lifetime of our systems.

Finally, we need to consider whether these simulations will eventually produce systems like the solar system. The instability that our multi-resonant planetary system suffers is quite likely to be more severe than that described in the original Nice model, given that the initial interplanetary separations are smaller in the present work. This was actually seen in Morbidelli et al. (2007) and Batygin & Brown (2010), who studied a large set of initial multi-resonant configurations, starting from the time where the planets were extracted from their resonances and until they effectively stopped migrating. The statistics of their final systems suggest that multi-resonant systems in which Jupiter and Saturn are initially in a 3:2 MMR, have a $\sim$10%–30% probability to evolve into a four-planet configuration that closely resembles our solar system. However, the exact success rate varies from initial configuration to initial configuration. Unfortunately, the configuration we chose to study in this paper is not among their best cases. It is thus clear that, in order to obtain proper statistics on final planetary systems, we would need to study several initial planetary configurations starting from the very beginning (as in the present paper), using a number of clones for each configuration and repeating for different values of the disk's mass. Given that each 1 Gyr simulation that includes viscous stirring takes *months* of CPU time, we decided to leave this matter for future work.

We note, however, that the exact way in which our unstable systems would evolve may be systematically different from those seen in previous simulations. This is because our planetesimal disk is still far from the planets, when the latter are extracted from their initial resonances. Thus, right after the instability sets in, encounters between planets and planetesimals are scarce and dynamical friction is weak. In the previous works the planets are "adiabatically" extracted from their resonances by encounters with planetesimals, hence their orbits are nearly circular when they leave their resonances. In our case, the multi-resonant state is suddenly broken by a secular resonance, and this leaves at least one planet (Ice I) with a significant eccentricity. Therefore, we cannot directly use the statistics from Morbidelli et al. (2007) and Batygin & Brown (2010), but must wait until the survey described in the last paragraph is complete.

4. CONCLUSIONS

In this paper, we have shown that a planet can irreversibly exchange energy with a planetesimal disk even in the absence of close encounters between planet and disk particles. We demonstrated that, for this to happen, it is essential that the viscous stirring in the disk is taken into account and the planet is eccentric. This energy exchange is related to a new form of gravitational friction that occurs through distant secular interactions and not through a process of scattering.

If the giant planets of the solar system got trapped in a multi-resonant configuration as a result of their convergent migration in the gas disk, the innermost ice giant (Ice I) is expected to have had an orbit with non-negligible eccentricity, unlike the other three planets (Morbidelli et al. 2007). In this configuration, Ice I would have lost energy if the system were surrounded by a planetesimal disk consisting, in part, of Pluto-mass objects. The resonances among the planets would have forced this energy decay to increase Ice I's eccentricity, thereby sustaining its energy exchange with the disk. Eventually, these modifications in orbital eccentricities might have turned the planetary system unstable. In our simulations, the giant planets become unstable after a time ranging between 300 Myr and 1 Gyr in $\sim$25% of the cases, for a wide range of disk masses and locations of the disk inner edge. This mechanism is therefore a powerful one to explain the late instability of the giant planet system, related to the trigger of the late heavy bombardment of the terrestrial planets.

Together, the paper by Morbidelli et al. (2007) and this new work, build a new version of the "Nice model." This new version, which we call Nice II, has distinct advantages over the original version (Tsiganis et al. 2005; Gomes et al. 2005) because: (1) it removes the arbitrary character of the initial conditions by adopting a planetary configuration derived from hydrodynamical simulations and (2) it removes the sensitive dependence of the instability time on the location of the inner edge of the disk. Indeed, a late instability seems to be a generic outcome.

Our new dynamical coupling may also have important implications for extra-solar systems as well. Many observed planetary systems contain planets in MMRs (Marois et al. 2008; Rivera et al. 2010) with one another, while others appear to have undergone a global dynamical instability (Ford et al. 2001; Matsumura et al. 2010). Our new coupling supplies a natural mechanism for driving resonant systems unstable—thereby turning the former into the latter.

REFERENCES

Barr, A. C., & Canup, R. M. 2010, Nat. Geosci., 3, 164
Batygin, K., & Brown, M. E. 2010, ApJ, 716, 1323
Bottke, W. F., Nesvorný, D., Vokrouhlický, D., & Morbidelli, A. 2010, AJ, 139, 994
Brasser, R., Morbidelli, A., Gomes, R., Tsiganis, K., & Levison, H. F. 2009, A&A, 507, 1053

Brown, M. E., & Schaller, E. L. 2007, Science, 316, 1585
Brown, M. E., Trujillo, C. A., & Rabinowitz, D. L. 2005, ApJ, 635, L97
Chambers, J. E., Wetherill, G. W., & Boss, A. P. 1996, Icarus, 119, 261
Duncan, M. J., Levison, H. F., & Lee, M. H. 1998, AJ, 116, 2067
Ford, E. B., Havlickova, M., & Rasio, F. A. 2001, Icarus, 150, 303
Gladman, B. 1993, Icarus, 106, 247
Goldreich, P., & Tremaine, S. 1980, ApJ, 241, 425
Goldreich, P., & Tremaine, S. 1982, ARA&A, 20, 249
Gomes, R., Levison, H. F., Tsiganis, K., & Morbidelli, A. 2005, Nature, 435, 466
Gomes, R. S., Morbidelli, A., & Levison, H. F. 2004, Icarus, 170, 492
Hartmann, W. K., Ryder, G., Dones, L., & Grinspoon, D. 2000, Origin of the Earth and Moon (Tucson, AZ: Univ. Arizona Press), 493
Henrard, J. 1993, Dynamics Reported, Vol. 2 (Berlin: Springer), 197
Levison, H. F., Bottke, W. F., Gounelle, M., et al. 2009, Nature, 460, 364
Levison, H. F., Morbidelli, A., Vanlaerhoven, C., Gomes, R., & Tsiganis, K. 2008, Icarus, 196, 258
Levison, H. F., Thommes, E., Duncan, M. J., & Dones, L. 2004, in ASP Conf. Ser. 324, Debris Disks and the Formation of Planets, ed. L. Caroff, L. J. Moon, D. Backman, & E. Praton (San Francisco, CA: ASP), 152
Malhotra, R. 1995, AJ, 110, 420
Marois, C., Macintosh, B., Barman, T., et al. 2008, Science, 322, 1348
Matsumura, S., Thommes, E. W., Chatterjee, S., & Rasio, F. A. 2010, ApJ, 714, 194
Milani, A., Nobili, A. M., & Carpino, M. 1987, A&A, 172, 265
Milani, A., Nobili, A. M., Fox, K., & Carpino, M. 1986, Nature, 319, 386
Morbidelli, A., Brasser, R., Gomes, R., Levison, H. F., & Tsiganis, K. 2010, AJ, 140, 1391
Morbidelli, A., Brasser, R., Tsiganis, K., Gomes, R., & Levison, H. F. 2009a, A&A, 507, 1041
Morbidelli, A., Levison, H. F., Bottke, W. F., Dones, L., & Nesvorný, D. 2009b, Icarus, 202, 310
Morbidelli, A., Levison, H. F., Tsiganis, K., & Gomes, R. 2005, Nature, 435, 462
Morbidelli, A., Tsiganis, K., Crida, A., Levison, H. F., & Gomes, R. 2007, AJ, 134, 1790
Nesvorný, D., Vokrouhlický, D., & Morbidelli, A. 2007, AJ, 133, 1962
Peale, S. J. 1986, in IAU Colloq. 77, Some Background about Satellites (Tucson, AZ: Univ. Arizona Press), 159
Pierens, A., & Nelson, R. P. 2008, A&A, 482, 333
Rauch, K. P., & Holman, M. 1999, AJ, 117, 1087
Rivera, E. J., Laughlin, G., Butler, R. P., et al. 2010, ApJ, 719, 890
Sheppard, S. S., & Trujillo, C. A. 2010, ApJ, 723, L233
Šidlichovský, M., & Nesvorný, D. 1996, Celest. Mech. Dyn. Astron., 65, 137
Stern, S. A. 1991, Icarus, 90, 271
Thommes, E. W., Duncan, M. J., & Levison, H. F. 1999, Nature, 402, 635
Thommes, E. W., Duncan, M. J., & Levison, H. F. 2003, Icarus, 161, 431
Tsiganis, K., Gomes, R., Morbidelli, A., & Levison, H. F. 2005, Nature, 435, 459
Wetherill, G. W., & Stewart, G. R. 1993, Icarus, 106, 190
Zhang, H., & Zhou, J.-L. 2010, ApJ, 714, 532